Available online at www.sciencedirect.com
ScienceDirect
Journal of Power Sources 168 (2007) 522–532
JOURNAL OF POWER SOURCES
www.elsevier.com/locate/jpowsour

Effect of metal-sulfide additives on electrochemical properties of nano-sized Fe_2O_3-loaded carbon for Fe/air battery anodes

Bui Thi Hang [a,*], Seong-Ho Yoon [b], Shigeto Okada [b], Jun-ichi Yamaki [b]

[a] *Japan Science and Technology Agency, Kasuga Koen 6-1, Kasuga 816-8580, Japan*
[b] *Institute for Materials Chemistry and Engineering, Kyushu University, Kasuga Koen 6-1, Kasuga 816-8580, Japan*

Received 13 December 2006; received in revised form 21 February 2007; accepted 23 February 2007
Available online 7 March 2007

Abstract

In the present study, K_2S and Bi_2S_3 were used as additives in electrolytes and electrodes, respectively. The effects of these additives on the electrochemical properties of nano-sized Fe_2O_3-loaded carbon electrodes were investigated using cyclic voltammetry (CV), galvanostatic cycling performance and scanning electron microscopy (SEM), along with electron dispersive spectroscopy (EDS). The results showed that both K_2S and Bi_2S_3 significantly reduced hydrogen evolution and benefited the Fe_2O_3-loaded carbon electrode, such as by retarding passivation and improving the discharge capacity. The effects of metal sulfide additives depended on the carbon used. For Bi_2S_3 additive, all carbons provided larger capacities than acetylene black (AB) while AB gave greater capacity than other carbons when K_2S was used.

Keywords: Nano-carbon; Metal-sulfide additive; Nano-sized Fe_2O_3-loaded carbon composite electrode; Iron/air battery anode

1. Introduction

There has recently been growing interest in porous iron electrodes since they have a high theoretical capacity (960 mAh g^{-1}) and a long cycle life, and are inexpensive and environment-friendly. However, a major problem with an iron electrode is passivation caused by iron hydroxide produced during discharge, which prevents further anodic utilization. Furthermore, a porous iron electrode has a low hydrogen overpotential, which limits its application in commercial batteries [1–5]. Numerous investigations have focused on improving the charging efficiency and discharge capacity, and minimizing self-discharge [1–16].

Although various metal sulfides (FeS, Bi_2S_3, Na_2S, K_2S, ...) have been used as additives with iron electrodes and associated electrolytes [2–21] to circumvent the above problems, their role is not yet fully understood. The effectiveness of a sulfide additive has been attributed to factors such as sulfide ion adsorption at the electrode/electrolyte interface, with subsequent incorporation into the oxide lattice [6–8], modification of the electrode kinetics [6], modification of the electrode texture and morphology [8], increase in the anodic current density [8–10], increase in the bulk electrode conductivity [2], enhanced rate of the $Fe/Fe(OH)_2$ reaction, increase in the solubility of iron compounds [4,8,10,17], and inhibition of self-discharge of the iron electrode [5,7,11]. Studies have shown that the addition of metal sulfides such as FeS, PbS, Bi_2S_3, or sulfur to the electrode active material [2,3,5,7–10,13,14,16] or Na_2S (or K_2S) to the KOH electrolytic solution [4,6,9,11,12,15,17–21] significantly increases the iron electrode capacity. In addition, LiOH has been used as an additive in KOH electrolyte [2,4–6,10,11,13–17] to improve the utility of the iron electrode. However, all of these metal sulfide additives were used for Fe electrode free carbon. Our previous work [22] revealed that an Fe/C mixed electrode improves the conductivity and redox current of an iron electrode and metal sulfide additives (K_2S and FeS) [23] had beneficial effects for an Fe/C mixed electrode, such as considerably suppressing hydrogen evolution and inhibiting passivation. To increase the surface area of the active material, nano-sized Fe_2O_3-loaded carbon was prepared [24]. This material provided larger capacity than mixed Fe/C. A disadvantage of nano-sized Fe_2O_3-loaded carbon was that passivation and hydrogen evolution still occurred during cycling. In the present study, K_2S and Bi_2S_3 were used as additives in nano-sized Fe_2O_3-loaded carbon to better understand their ability to promote depassivation

* Corresponding author. Tel.: +81 92 583 7790; fax: +81 92 583 7790.
E-mail address: hang@cm.kyushu-u.ac.jp (B.T. Hang).

0378-7753/$ – see front matter © 2007 Elsevier B.V. All rights reserved.
doi:10.1016/j.jpowsour.2007.02.067

and reduce hydrogen evolution and thereby improve the cycle performance.

2. Experimental

Vapor-grown carbon fibers (VGCF; Showa Denko Co.), acetylene black (AB, Denki Kagaku Co.) and natural graphite (Chuetsu Graphite Co.), with average diameters of ca. 200 nm, 100 nm and 18 μm, respectively, were used in the present work. In addition, two kinds of carbon nanofibers (CNFs), a nanotube type, with an average diameter of ca. 50 nm, and a platelet type, with an average diameter of ca. 150 nm, were also investigated. For tubular CNF, graphene is aligned parallel to the fiber axis while in platelet CNF graphene is aligned perpendicular to the fiber axis. The main characteristics and morphology of the carbon materials used have been described previously [22]. Iron nitrate (Wako Pure Chemical, Co.) was used as the iron source.

The Fe_2O_3-loaded carbon material was prepared by impregnating $Fe(NO_3)_3$ on carbon with an iron to carbon weight ratio of 1:8 in an aqueous solution. The mixture was then dried at 70 °C, followed by calcination for 1 h at 400 °C in flowing Ar. The Fe compound obtained on the carbons was identified to be Fe_2O_3 by X-ray diffraction. The morphology of the as-prepared Fe_2O_3-loaded carbon materials was observed by transmission electron microscopy (TEM) and scanning electron microscopy (SEM), together with X-ray energy dispersive spectroscopy (EDS).

To determine the electrochemical behavior of each Fe_2O_3-loaded carbon material, electrodes with and without Bi_2S_3 additive were prepared. An electrode sheet free of additive was prepared by mixing 90 wt% of the respective Fe_2O_3-loaded carbons and 10 wt% polytetrafluoroethylene (PTFE; Daikin Co.),

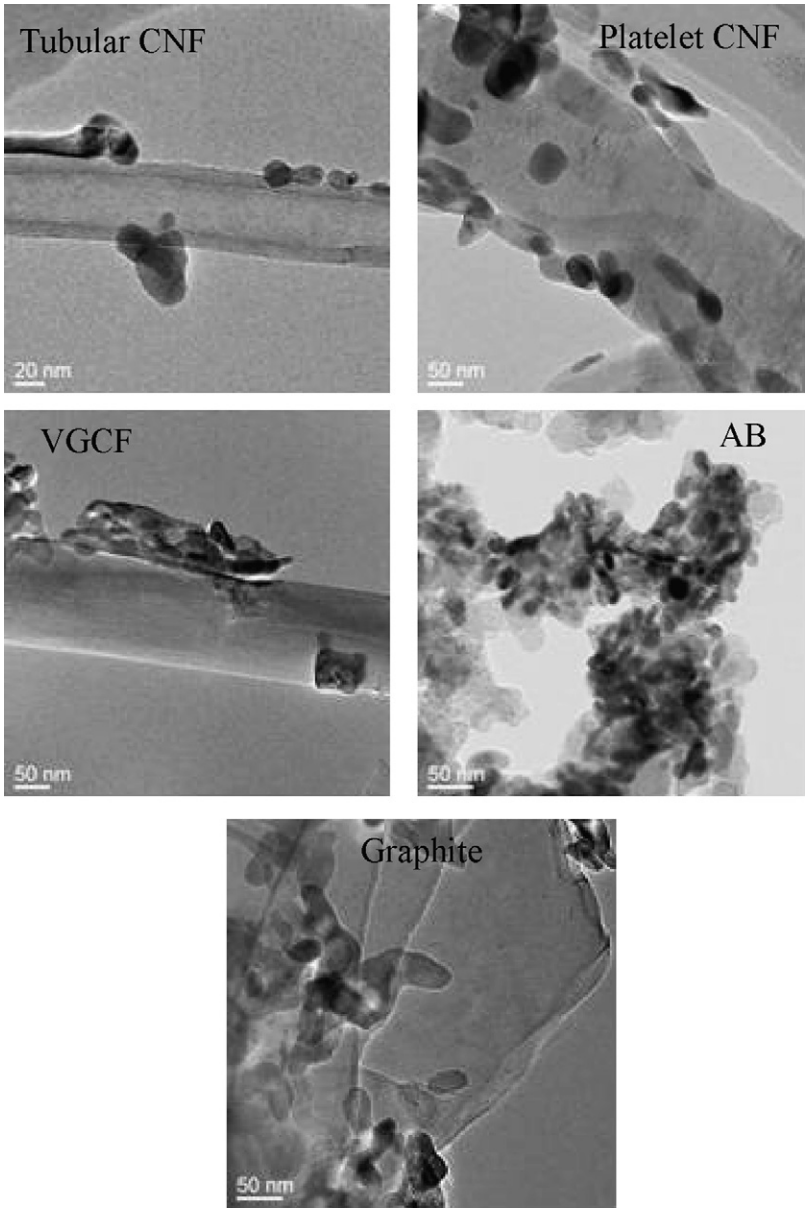

Fig. 1. TEM images of nano-sized Fe_2O_3-loaded carbon using various carbon materials.

and rolling. Electrodes containing Bi_2S_3 additive were prepared by the same procedure. Bi_2S_3, which was present at two levels in the Fe_2O_3-loaded carbon electrode, 1 wt% and 2 wt%, was incorporated into the electrodes by mixing before rolling. The Fe_2O_3-loaded carbon electrode was made into a pellet 1 cm in diameter. Two kinds of electrolyte were prepared: additive-free (base electrolyte) and containing additive. The base electrolyte was 8 mol dm^{-3} aqueous KOH solution, and the additive electrolyte was KOH solution containing 0.05 M and 0.1 M of K_2S (total concentration of KOH and K_2S was 8 M). Cyclic voltammetry studies were carried out with a three-electrode glass cell assembly that had an Fe_2O_3-loaded carbon electrode as the working electrode, silver oxide as the counter electrode, Hg/HgO (1 M NaOH) as the reference electrode and cellophane together with filter paper as a separator, which was sandwiched by the two electrodes. The base electrolyte was used for electrodes with Bi_2S_3 additive, and the electrolyte containing K_2S was used for sulfide-free electrodes. Cyclic voltammetry measurements were recorded at a sweep rate of 0.5 mV s^{-1} and within a range of −1.3 V to −0.1 V. After the 15th and 50th redox cycles, the Fe_2O_3-loaded carbon electrodes were removed, washed with deionized water, dried and observed by SEM-EDS for comparison with the findings before cycling.

Galvanostatic cycling performance for the Fe_2O_3-loaded carbon electrodes was measured with a three-electrode glass cell assembly. The discharge cutoff potential was −0.1 V, and a constant potential charging step was applied at −1.15 V after galvanostatic charging. A constant potential of −1.15 V was used because of the large amount of hydrogen evolution observed at −1.2 V. The current densities for the charge and discharge processes were 0.5 mA cm^{-2} and 0.2 mA cm^{-2}, respectively.

3. Results and discussion

The Fe compound obtained on the carbons was identified to be Fe_2O_3 by X-ray diffraction [24]. Thus, the active material in this case is Fe_2O_3.

TEM images of as-prepared Fe_2O_3-loaded carbon using various carbon materials are shown in Fig. 1. The dark particles in these pictures are Fe_2O_3. The TEM images indicated that fine Fe_2O_3 particles were dispersed on the carbon surface. The particle size of Fe_2O_3 is about a few tenths of a nanometer. Such a distribution of Fe_2O_3 is expected to improve the cycleability of Fe_2O_3-loaded carbon electrodes.

Fig. 2 depicts SEM images and the distribution of iron and carbon by EDS of as-prepared nano-sized Fe_2O_3-loaded materials using graphite and tubular CNF, respectively. The distribution of iron and carbon on nano-sized Fe_2O_3-loaded graphite and tubular CNF materials revealed that iron pieces were well dispersed on the carbon surface. Such distribution should increase

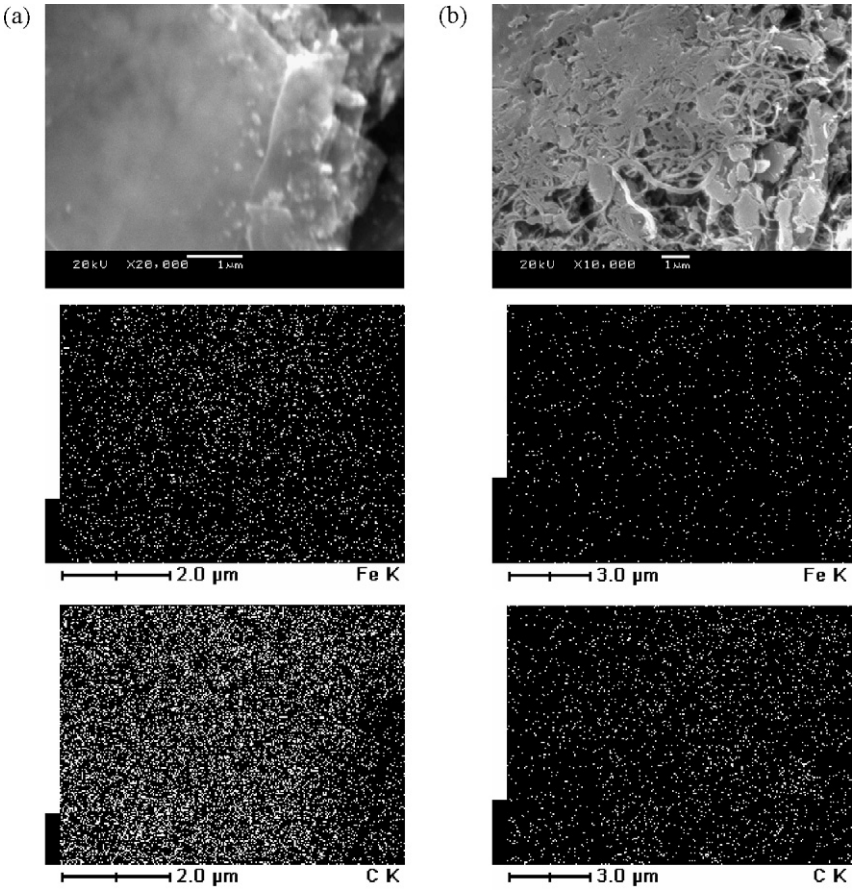

Fig. 2. SEM images and distribution of Fe and carbon for nano-sized Fe_2O_3-loaded (a) graphite and (b) tubular CNF material.

the surface area of active material and improve the cycle performance of nano-sized Fe_2O_3-loaded carbon electrodes.

Voltammograms of nano-sized Fe_2O_3-loaded carbon electrodes in base electrolyte and in electrolyte containing 0.1 M of the K_2S additive as well as the electrode with 1 wt% of Bi_2S_3 additive after the first five cycles are shown in Figs. 3 and 4. In the case of nano-sized Fe_2O_3-loaded electrodes without additive (Figs. 3a and 4a), a couple redox reaction peak was observed at around −0.6 V (a_2) upon oxidation and at around −1.0 V (c_1) upon reduction. The form of carbon affected the redox behavior of the electrodes. For example, tubular CNF, AB and graphite provided a sharp couple peak while the peaks were rather small for platelet CNF or VGCF. With repeated cycling, the anodic peak moved toward a more positive potential and the cathodic peak shifted to a more negative potential, especially in the case of AB and platelet CNF. In the literature [1,2,17–19], the overall electrochemical behavior involved in the passivation and dissolution of iron in alkaline solution has been proposed to consist of two main steps, the first of which is [1]

$$Fe + 2OH^- \rightleftarrows Fe(OH)_2 + 2e, \quad E^0 = -0.975\,V \tag{1}$$

According to some authors [17–19], Eq. (1) involves the following partial steps in conjunction with the adsorption of OH^- ion:

$$Fe + OH^- \rightleftarrows [Fe(OH)]_{ad} + e \tag{2}$$

$$[Fe(OH)]_{ad} + OH^- \rightleftarrows Fe(OH)_2 + e \tag{3}$$

Most authors agree that the formation of $Fe(OH)_2$ proceeds through the formation of the soluble intermediate product, $HFeO_2^-$ [1,15], the concentration of which is strongly temperature-dependent [17–19], i.e.:

$$[Fe(OH)]_{ad} + 2OH^- \rightleftarrows HFeO_2^- + H_2O + e \tag{4}$$

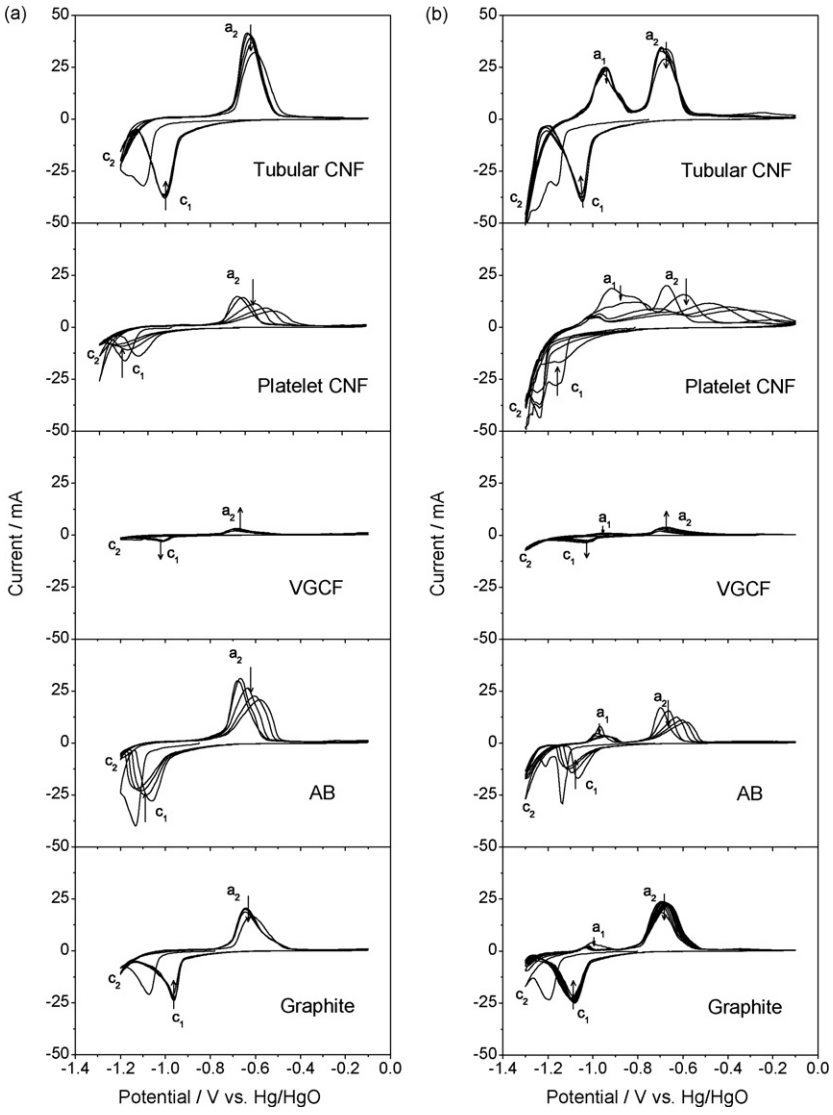

Fig. 3. Cyclic voltammetry for Fe_2O_3-loaded carbon composite electrodes in (a) base electrolyte and (b) electrolyte containing 0.1 M K_2S additive after the five initial cycles. (Arrows indicate the tendency of the current during cycling.)

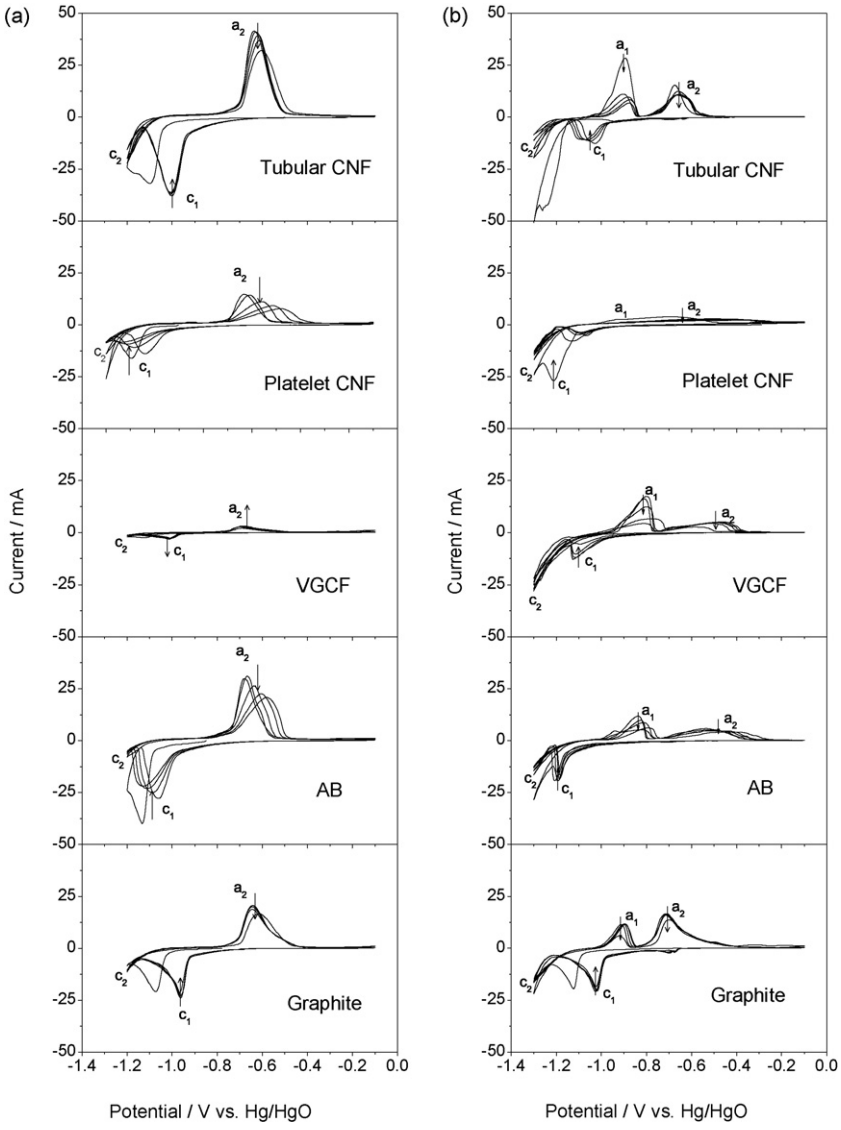

Fig. 4. Cyclic voltammetry for Fe_2O_3-loaded carbon composite electrodes (a) without and (b) with 1 wt% Bi_2S_3 additive after the five initial cycles in base electrolyte. (Arrows indicate the tendency of the current during cycling.)

and

$$HFeO_2^- + H_2O \rightleftarrows Fe(OH)_2 + OH^- \quad (5)$$

The second oxidation step of the iron electrode involves [1]

$$Fe(OH)_2 + OH^- \rightleftarrows FeOOH + H_2O + e, \quad E^0 = -0.658\,V \quad (6)$$

and/or [13,14]

$$3Fe(OH)_2 + 2OH^- \rightleftarrows Fe_3O_4{\cdot}4H_2O + 2e, \quad E^0 = -0.758\,V \quad (7)$$

Thus, anodic peak a_2 involves the oxidation of both Fe to Fe(II) (Eq. (1)) and Fe(II) to Fe(III). In the first scan, Fe(II) was converted to Fe(III) as shown by Eqs. (6) and (7), however, from the second scan, the oxidation of Fe(II) only proceeded via Eq. (7), as evidenced by the Fe_3O_4 production including Fe(II) and Fe(III). Cathodic peak c_1 corresponds to the reduction of both Fe(III)/Fe(II) and Fe(II)/Fe. The first anodic peak a_1 (Eq. (1)) did not appear separately from anodic peak a_2 due to the formation of a passive layer, caused by the reaction of nano-sized Fe_2O_3.

From Figs. 3 and 4, it is clear that K_2S and Bi_2S_3 as additives strongly affect the redox behavior of iron. When these metal sulfide additives were used with all of the carbons tested (Figs. 3b and 4b), with both K_2S and Bi_2S_3, along with the appearance of a redox couple peak a_2–c_1, a new oxidation peak a_1 occurred at around −0.95 V. The anodic peak a_1 is attributed to the oxidation of Fe to Fe(II) (Eq. (1)), which causes the passivation of iron electrode. In the presence of K_2S or Bi_2S_3 additive, the anodic peak a_1 increased, which means that the reaction rate of Eq. (1) was increased. This suggests that passivation was retarded by the sulfide ion. This result agrees with those in previous reports [4–6,8,17,21]. S^{2-} additive was thought to adsorb at the electrode/electrolyte interface and then be incor-

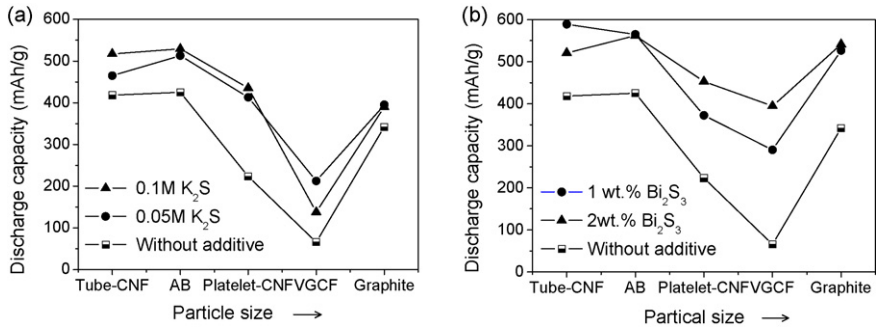

Fig. 5. Dependence of the discharge capacity of Fe_2O_3-loaded carbon at the fifth cycle on the carbon material and either the (a) K_2S concentration in additive-containing electrolyte or (b) Bi_2S_3 content for Fe_2O_3-loaded carbon electrodes with Bi_2S_3 additive.

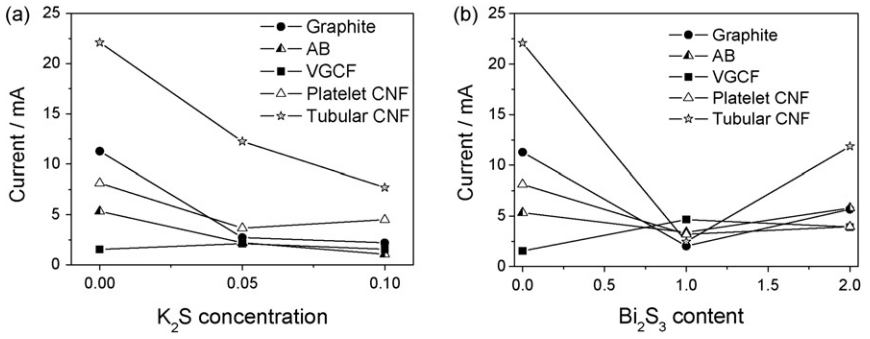

Fig. 6. Variation of the hydrogen evolution current of Fe_2O_3-loaded carbon electrodes in the fifth cycle with (a) the K_2S concentration in additive-containing electrolyte and (b) the Bi_2S_3 content for Fe_2O_3-loaded carbon electrodes with Bi_2S_3 additive at −1.2 V.

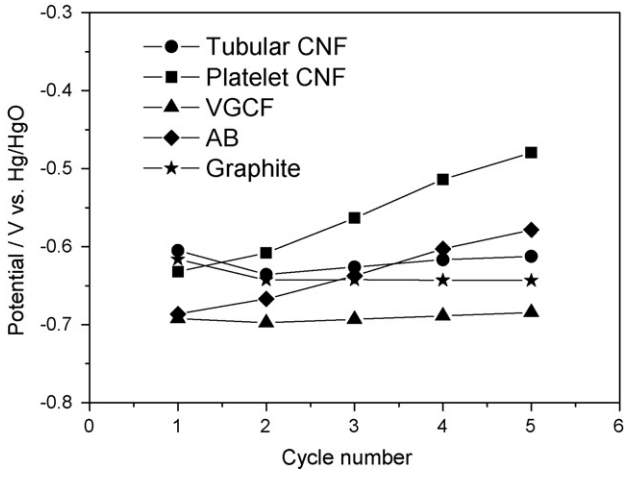

Fig. 7. Variation of oxidation peak a_2 of Fe_2O_3-loaded carbon electrodes without additive.

porated into the $Fe(OH)_2$ lattice [6–8], which would modify the electrode texture and morphology [8] to distort the oxide film, which leads to an increase in the ionic conductivity of the passive layer [10] and enhances the rate of the $Fe/Fe(OH)_2$ reaction [4,8,10,17]. Obviously, this retards the passivation process and a thicker film is formed. Thus, the presence of K_2S or Bi_2S_3 in the electrolyte or electrode, respectively, favored de-passivation of the electrode. With further cycling, peak a_1 was decreased and the overpotential of the couple peak a_2–c_1 was increased, which means that re-passivation occurred. The anodic peaks that occurred at a potential higher than −0.5 V may be due to side reactions caused by the adsorbed S^{2-} [20].

To evaluate the effect of metal sulfide additives on nano-sized Fe_2O_3-loaded carbon electrodes, the discharge capacity and hydrogen evolution of electrodes without and with the additives were calculated from CV measurements at the 5th cycle in Figs. 3 and 4, and the results are presented in Figs. 5 and 6,

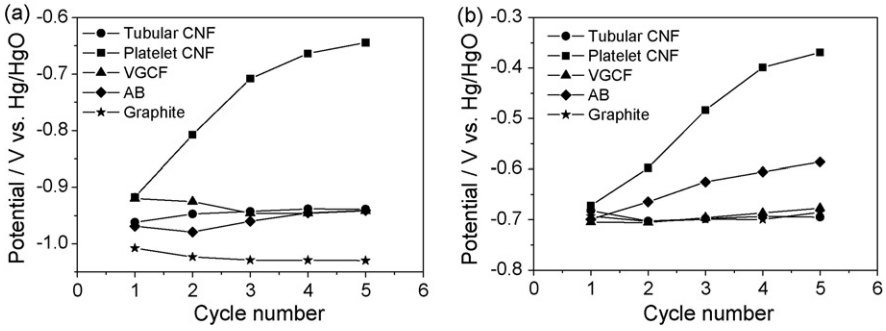

Fig. 8. Variation of oxidation peaks (a) a_1 and (b) a_2 of Fe_2O_3-loaded carbon electrodes in electrolyte containing 0.1 M K_2S additive with cycle number.

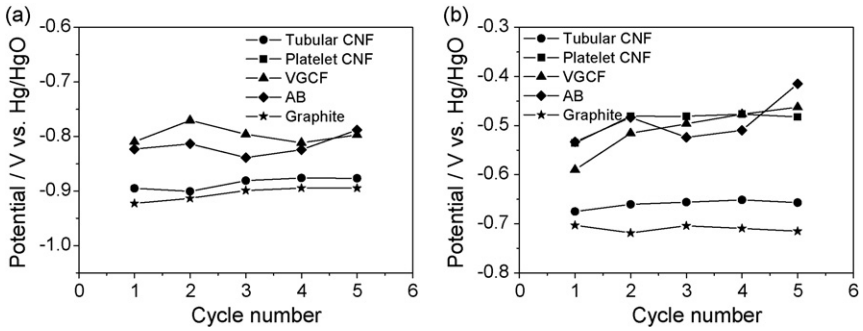

Fig. 9. Variation of oxidation peaks (a) a_1 and (b) a_2 of Fe_2O_3-loaded carbon electrodes containing 1 wt% Bi_2S_3 additive with cycle number.

respectively. Discharge capacity was calculated from the total areas of anode peaks ($a_1 + a_2$) and hydrogen evolution was taken from the current value at −1.2 V. Regarding discharge capacity (Fig. 5) without additive, nano-sized Fe_2O_3-loaded tubular CNF and AB provided greater capacities than other carbons. This is reasonable, since nano-carbons, especially tubular CNF and AB, have greater actual surface areas than other carbons. Consequently, Fe_2O_3 was more dispersed on tubular CNF and AB than on other carbons. Such dispersion results in a larger active surface area for Fe_2O_3-loaded tubular CNF and AB electrodes than for other Fe_2O_3-loaded carbon electrodes, thereby supporting the redox reaction of iron. With the use of a metal sulfide additive, the discharge capacities of nano-sized Fe_2O_3-loaded carbon electrodes were remarkably improved (Fig. 5). The effect of an additive depended on the type of carbon, the type of additive and the concentration of the additive. Bi_2S_3 had a more beneficial effect than K_2S, as evidenced by greater capacities for all of the carbons. Among the carbons used, electrodes with tubular CNF and AB delivered larger discharge capacities than those of other carbons when K_2S or Bi_2S_3 was used. Interestingly, the electrode using graphite delivered as large as a capacity as those containing tubular CNF or AB in the presence of Bi_2S_3 additive. Particularly, the discharge capacity of VGCF was less than that of other carbons, and was increased considerably by Bi_2S_3 additive.

On the other hand, the role of additive in the hydrogen evolution reaction is an important factor that contributes to improving the cycle performance of electrode. Two paths for the hydrogen electrode evolution in alkaline solution were considered [21]:

a primary step:

$$H_2O + e \rightarrow H_{ad} + OH^- \quad \text{(I)}$$

coupled with either an electrochemical desorption step:

$$H_2O + H_{ad} + e \rightarrow H_2 + OH^- \quad \text{(II)}$$

or a molecular recombination desorption step:

$$H_{ad} + H_{ad} \rightarrow H_2 \quad \text{(III)}$$

The variation of current, which was attributed to hydrogen evolution at −1.2 V, with the concentration of the additive is depicted in Fig. 6. Compared with the additive-free electrodes, hydrogen evolution was greatly decreased for all of the carbons

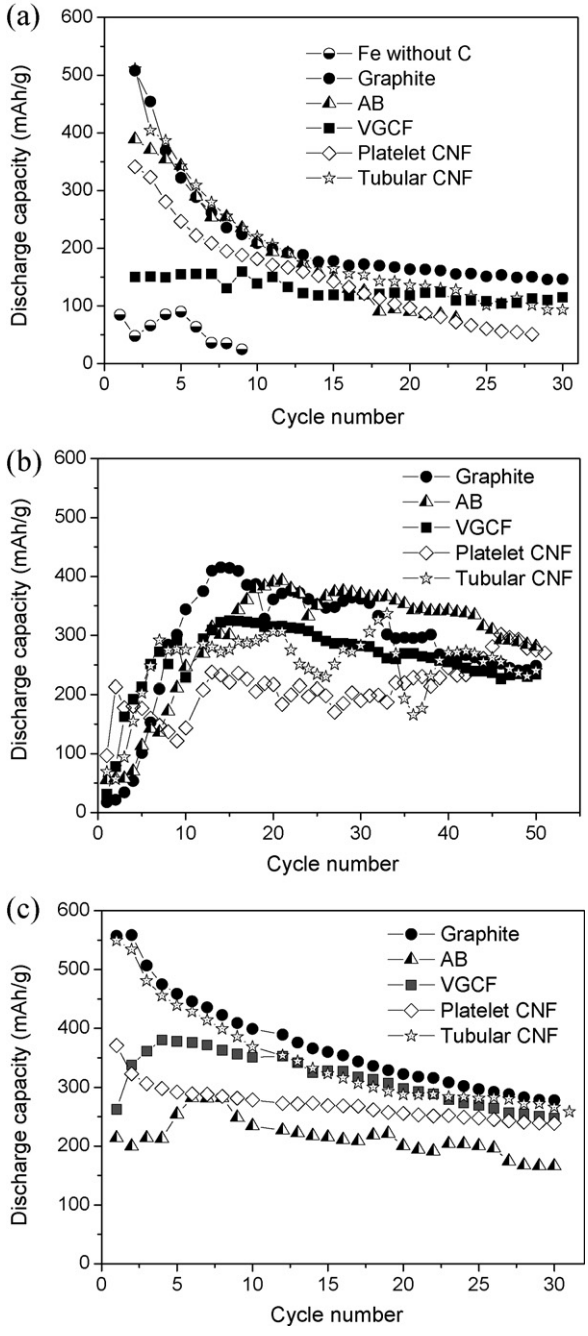

Fig. 10. Cycle performance of electrodes (a) without additive, (b) with 0.1 M K_2S additive in the electrolyte, or (c) 2 wt% Bi_2S_3 additive in the electrode.

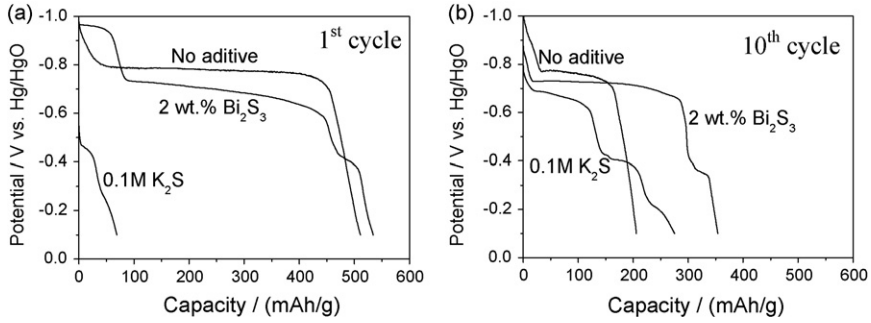

Fig. 11. Discharge curves of nano-sized Fe_2O_3-loaded tubular CNF without and with additive.

tested. It is clear that hydrogen evolution was significantly suppressed by both K_2S and Bi_2S_3 additive for all of the carbons. This result agrees with those reported earlier [7,14,20]; the main reason for this result is absorption of the highly polarizable S^{2-} ion. Carta et al. [21] claimed that the molecular recombination reaction (step (III)) was inhibited by S^{2-} ion chemisorption. Another possible reason is that the change in surface species probably also influences the overpotential of the hydrogen evolution reaction [18].

In addition to the above effects of metal sulfide additives, the position of redox peaks was changed in the presence of additive. The variation of anodic peaks of electrodes with and without additive is presented in Figs. 7 and 8. The oxidation peak a_2 of additive-free electrode (Fig. 7) gradually moved to a more positive potential with repeated cycling when AB, platelet CNF or VGCF was used. This suggested that overpotential was gradually increased, which led to a decrease in capacity. For tubular CNF or graphite, this peak seems to be maintained on

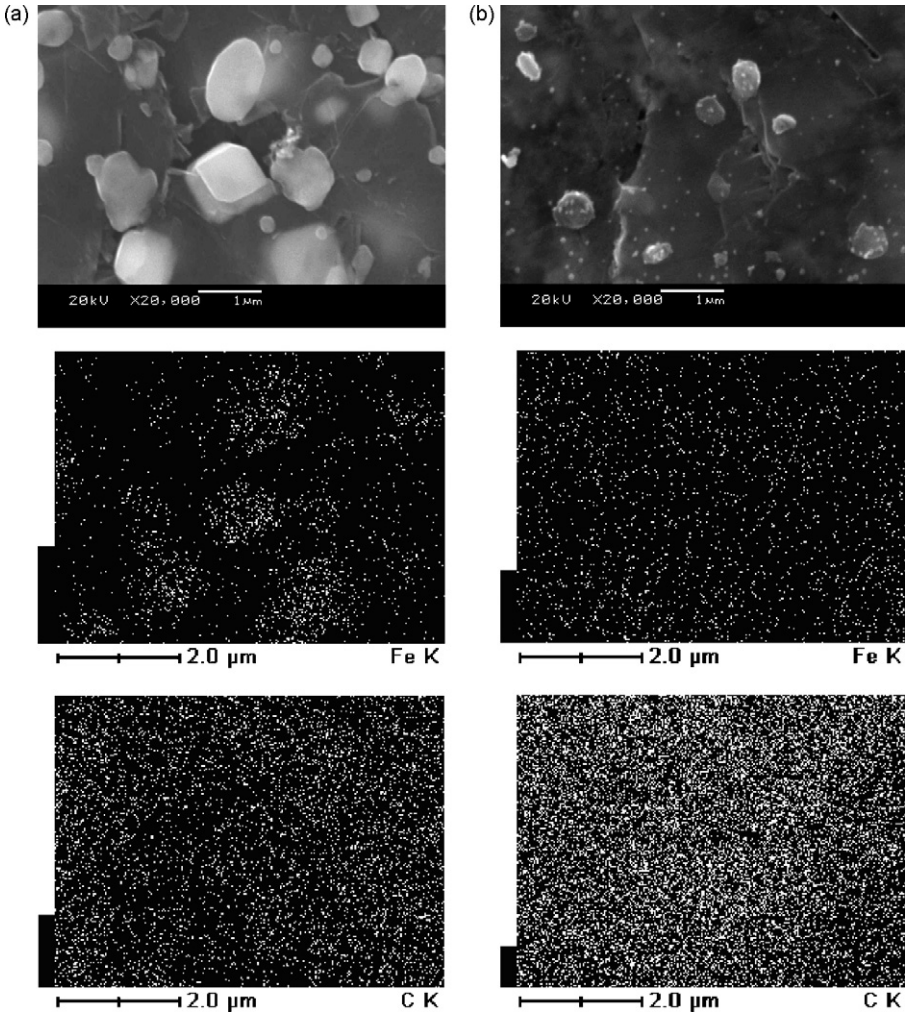

Fig. 12. SEM images and distribution of Fe and carbon for nano-sized Fe_2O_3-loaded graphite (a) without additive and (b) with 0.1 M K_2S additive in the electrolyte after the 15th cycle.

subsequent sweeping. This tendency was accelerated by K_2S or Bi_2S_3 additive not only at anodic peak a_2 but also at a_1 (Figs. 8 and 9). This leads to an increase in overpotential and overlap of the oxidation peak of iron and a side reaction at high potential. The reactions that appeared at potential higher than −0.5 V are attributed to side reactions due to the oxidation of S^{2-} adsorption [20].

The cycle performance of nano-sized Fe_2O_3-loaded carbons without and with additive is shown in Fig. 10. For additive-free electrodes, high discharge capacities were obtained at initial cycles and these gradually decreased in subsequent cycles (Fig. 10a). Cycle performance was significantly improved when a metal sulfide additive was used (Fig. 10b and c). The effect of the additive depended on the type of carbon and the additive. In the case of Bi_2S_3 (Fig. 10c), while the trend in the change in discharge capacity is similar to that of the additive-free electrode the discharge capacity values themselves are much higher. This is attributed to the effect of S^{2-} adsorption, as discussed in the description of CV measurement. Although the cycle performance of electrodes was improved by Bi_2S_3, the discharge capacity still gradually decreased with repeated cycling, and graphite, tubular CNF and VGCF provided greater discharge capacities than AB or platelet CNF. A quite different result was seen when K_2S was used (Fig. 10b). In initial cycles, the discharge capacity was very small but then gradually increased to reach high capacity after about 15 cycles; however, this value gradually decreased with further cycling. This result may be due to too much S^{2-} ion in the electrolyte with the use of 0.1 M K_2S. The surface of the electrode was fully covered by adsorbed S^{2-} at the beginning of the cycling, which led to a very low reaction rate of iron pieces. This caused a small capacity for the electrode in the initial cycles. Upon further cycling, adsorbed S^{2-} was consumed in part due to the oxidation of sulfide ion [20] and the remaining adsorbed S^{2-} supported the Fe/Fe(II) reaction to result in an increase in the discharge capacity. This was confirmed by the discharge curves of electrode using tubular CNF in Fig. 11. In the first cycle (Fig. 11a), one plateau was observed with an additive-free electrode at around −0.8 V and two plateaus occurred at around −0.95 V and −0.75 V when Bi_2S_3 was used. For K_2S additive, no plateau was seen within the range of −1.0 V to −0.7 V, except for a small plateau at around −0.45 V, which is attributed to a side reaction of sulfide ion. When the cycle number increased to the 10th cycle (Fig. 11b), a plateau was seen around −0.7 V along with an

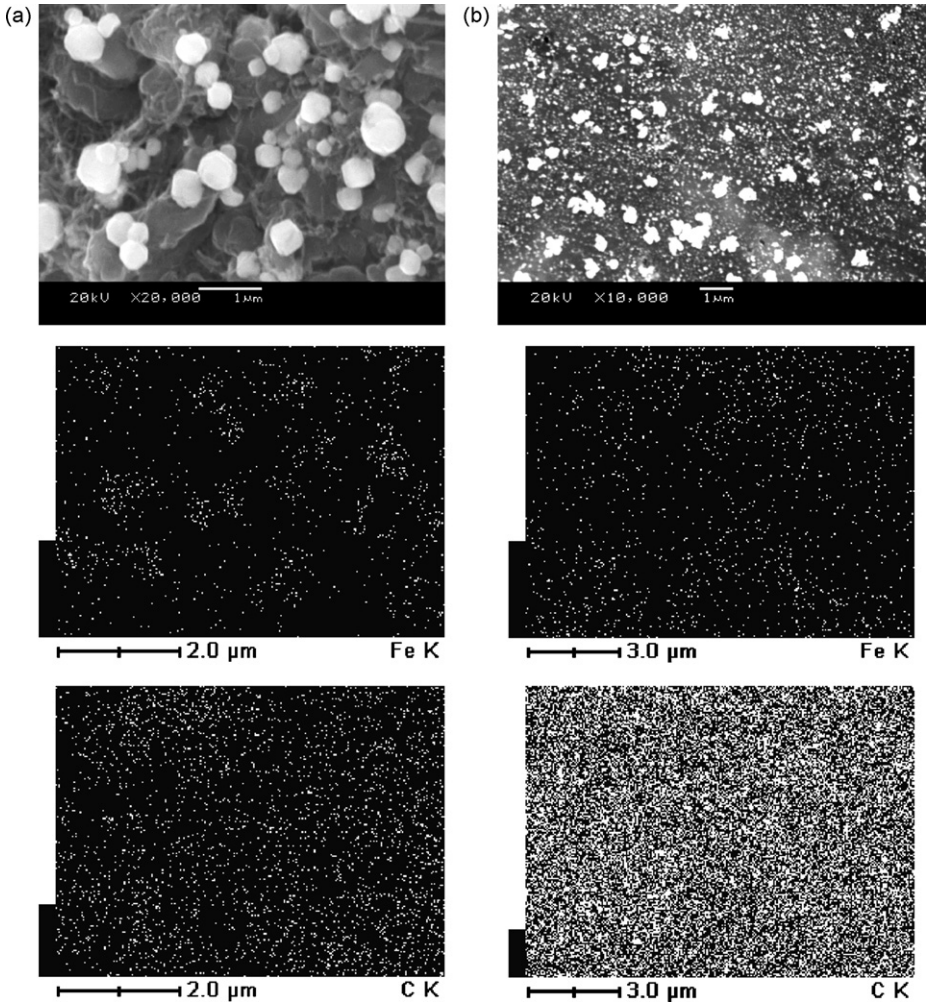

Fig. 13. SEM images and distribution of Fe and carbon for nano-sized Fe_2O_3-loaded tubular CNF (a) without additive and (b) with 2 wt% Bi_2S_3 additive in the electrode after the 15th cycle.

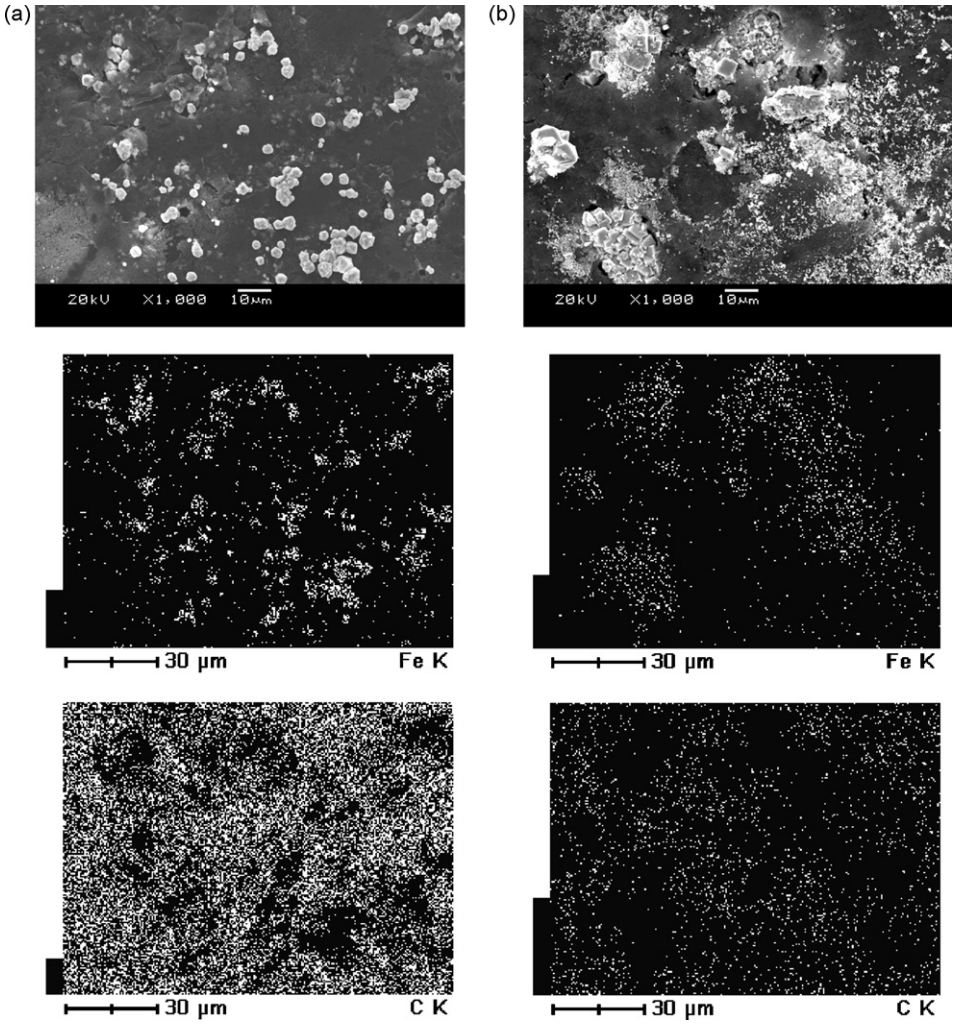

Fig. 14. SEM images and distribution of Fe and carbon for nano-sized Fe_2O_3-loaded (a) graphite in electrolyte containing 0.1 M K_2S additive and (b) tubular CNF with 2 wt% Bi_2S_3 additive in the electrode after the 50th cycle.

increase in discharge capacity in the case of K_2S additive, while a large capacity was maintained for Bi_2S_3 additive even though it gradually decreased. Thus, the beneficial effect of a sulfide additive was clearly revealed by the larger capacity of an electrode containing additive compared to that of an additive-free electrode.

To better understand why the cycle performance improved with a metal sulfide additive as well as the decrease in capacity with repeated cycling even in presence of additive, SEM and EDS studies were carried out on electrodes with and without additive after the 15th cycle and the results are presented in Figs. 12 and 13. Compared to SEM and EDS results before cycling (Fig. 2), it is clear that after cycling, in the case of without additive (Figs. 12a and 13a), iron was aggregated into large particles on the carbon surface, and this could explain the disappearance of the first anodic peak a_1 in the CV measurement (Fig. 3a) and the decrease in discharge capacity upon further cycling (Fig. 10a). When additive was applied to an electrode or electrolyte, after the 15th cycle, iron pieces were still distributed uniformly (Figs. 12b and 13b). Such distribution of iron pieces favored the redox reaction of iron and retarded the passivation process, which led to an increase in the capacity of the electrode (Fig. 10b and c). This result is consistent with the CV measurement, as evidenced by the appearance of anodic peak a_1, which is attributed to the oxidation of $Fe/Fe(OH)_2$. However, if cycling was prolonged until the 50th cycle, the distribution of iron changed (Fig. 14): large iron particles were observed on the carbon surface even in the presence of additive. This is thought to be one of the main causes of the decline in capacity. This decrease may also be promoted by side reactions caused by the additive. The oxidation of sulfide ion leads to repassivation of the electrode by the deposition of elemental sulfur [20].

4. Conclusions

The effects of K_2S and Bi_2S_3 additives on the electrochemical behavior of nano-sized Fe_2O_3-loaded carbon electrodes were interpreted in terms of the adsorbed sulfide ion. Ion sulfide is incorporated into the $Fe(OH)_2$ lattice and interacts with Fe(II) in the oxide film to enhance the ionic conductivity of the electrode, retard passivation and promote the dissolution of iron, which improve the cycle performance.

Sulfide may also suppress hydrogen evolution. A significant reduction in hydrogen evolution was attributed to inhibition of the molecular recombination reaction of hydrogen adsorption by S^{2-} ion chemisorption.

The effects of additives on the cycle performance of nano-sized Fe_2O_3-loaded carbon depend on the type of carbon used as well as the additive. The discharge capacity of nano-sized Fe_2O_3-loaded carbon electrode was remarkably improved by both K_2S and Bi_2S_3. Bi_2S_3 had a greater benefit than K_2S additive for all of the carbons tested in terms of capacity. In the presence of metal sulfide additive, nano-sized Fe_2O_3-loaded carbon is a promising candidate for a high-capacity Fe-air battery anode.

Acknowledgement

This work was supported by the CREST program of JST (Japan Science & Technology Agency).

References

[1] C. Chakkaravarthy, P. Perasamy, S. Jegannathan, K.I. Vasu, J. Power Sources 35 (1991) 21–35.
[2] K. Vijayamohanan, A.K. Shukla, J. Power Sources 32 (1990) 329–339.
[3] J. Cerny, J. Power Sources 45 (1993) 267–279.
[4] P. Periasamy, B.R. Babu, S.V. Iyer, J. Power Sources 63 (1996) 79–85.
[5] C.A.C. Souza, I.A. Carlos, M.C. Lopes, G.A. Finazzi, M.R.H. de Almeida, J. Power Sources 132 (2004) 288–290.
[6] N.A. Hampson, R.J. Latham, A. Marshall, R.D. Giles, Electrochim. Acta 19 (1974) 397–401.
[7] L. Ojefors, Electrochim. Acta 21 (1976) 263–266.
[8] K. Vijayamohanan, A.K. Shukla, S. Sathyanarayana, J. Electroanal. Chem. 289 (1990) 55–68.
[9] K. Micka, Z. Zabransky, J. Power Sources 19 (1987) 315–323.
[10] C.A. Caldas, M.C. Lopes, I.A. Carlos, J. Power Sources 74 (1998) 108–112.
[11] P.R. Vassie, A.C.C. Tseung, Electrochim. Acta 21 (1976) 299–302.
[12] M. Jayalakshmi, B.N. Begumi, V.R. Chidambaram, R. Sabapathi, V.S. Muralidharan, J. Power Sources 39 (1992) 113–119.
[13] K. Vijayamohanan, A.K. Shukla, S. Sathyanarayana, J. Electroanal. Chem. 295 (1990) 59–70.
[14] T.S. Balasubramanian, A.K. Shukla, J. Power Sources 41 (1993) 99–105.
[15] P. Periasamy, B.R. Babu, S.V. Iyer, J. Power Sources 58 (1996) 35–40.
[16] P. Periasamy, B.R. Babu, S.V. Iyer, J. Power Sources 62 (1996) 9–14.
[17] G.P. Kalaignan, V.S. Muralidharan, K.I. Vasu, J. Appl. Electrochem. 17 (1987) 1083–1092.
[18] R.S. Schrebler-Guzman, J.R. Viche, A.J. Arvia, Electrochim. Acta 24 (1979) 395–403.
[19] J. Cerny, K. Micka, J. Power Sources 25 (1989) 111–122.
[20] D.W. Shoesmith, P. Taylor, M.G. Bailey, B. Ikeda, Electrochim. Acta 23 (1978) 903–916.
[21] R. Carta, S. Dernini, A.M. Polcaro, P.F. Ricci, G. Tola, J. Electroanal. Chem. 257 (1988) 257–268.
[22] T.H. Bui, M. Egashira, I. Watanabe, S. Okada, J. Yamaki, S. Yoon, I. Mochida, J. Power Sources 143 (2005) 256–264.
[23] B.T. Hang, T. Watanabe, M. Eashira, I. Watanabe, S. Okada, J. Yamaki, J. Power Sources 155 (2006) 461–469.
[24] B.T. Hang, T. Watanabe, M. Eashira, S. Okada, J. Yamaki, S. Hata, S. Yoon, I. Mochida, J. Power Sources 150 (2005) 261–271.